

DEVELOPMENT OF AN OPTICAL BEAM PROFILE MONITOR FOR THE HZB CYCLOTRON

A. Denker[†], A. Akin, J. Bundesmann, A. Dittwald, T. Fanselow, I. Ja, M. Kang, G. Kourkafas
Helmholtz-Zentrum Berlin für Materialien und Energie, Berlin, Germany

Abstract

The HZB cyclotron accelerator complex provides 68 MeV protons for proton therapy and related research. The main accelerator is an isochronous sector cyclotron served by two injectors. Originally, the cyclotron was designed for heavy ions. Hence, the beam profile monitors (BPM) on the high energy side are not appropriate for protons at the low intensities used for proton therapy. At the experimental station as well as the treatment station, the profile and shape of the beam is determined via a mirrored image of a scintillator screen in air. For the experimental station, a LabVIEW code has been developed which displays the shape, transverse beam distribution, size and position of the beam. As this tool proved to be very helpful when tuning the beam for experiments, an installation within the beam line in vacuum was designed for several locations where the beam is focused. The design of the new beam profile monitors and their performance will be presented.

INTRODUCTION

The HZB cyclotron can provide both light and heavy ions over a broad energy range [1]. In the past, mainly heavy ions with energies between 1 MeV/u to 10 MeV/u have been used. Only a small amount of beamtime was used for light ions. For this reason, the BPMs in the high-energy beamline of the cyclotron were designed for heavy ions. They consist of a rotating wire which require a certain intensity to provide a good signal. The special development for low intensities [2] proved to be too sensitive for regular operation. Nowadays the main use of the cyclotron is ocular tumour therapy with 68 MeV protons and a typical intensity below 30 nA [3]. At these energies, the thin wires become transparent for the proton beam, and the signal of the BPM is overwhelmed by noise. Based on the excellent experience of the 2D cameras used at the experimental station [4], new optical BPMs have been developed and installed. The need for new BPMs arises due to the installation of two new dedicated beamlines, one for radiation hardness tests and one for minibeam experiments, the project MINIBEE [5,6].

LAYOUT

The camera and the objective of the BPMs are outside the vacuum pipe, looking through a CF35 glass window onto the scintillating material which is tilted 45° versus the

beam direction (Fig. 1). The camera lens is held by an adjustable tripod, fixed by a 3D printed holder. The shielding against stray light is also 3D printed. The scintillating material is mounted on a CF16 linear manipulator (Allectra GmbH [7]) which permits placing the BPM in the beam or outside of the beam. Limit switches not only supervise the position of the BPM but are also used for powering/depowering the camera to minimize radiation damages to the camera.

At the bottom is the holder for the scintillating material, tilted at 45° with respect to the beam axis. The size of the scintillator visible by the camera is 20 mm x 20 mm.

The whole system is mounted on a CF100 flange.

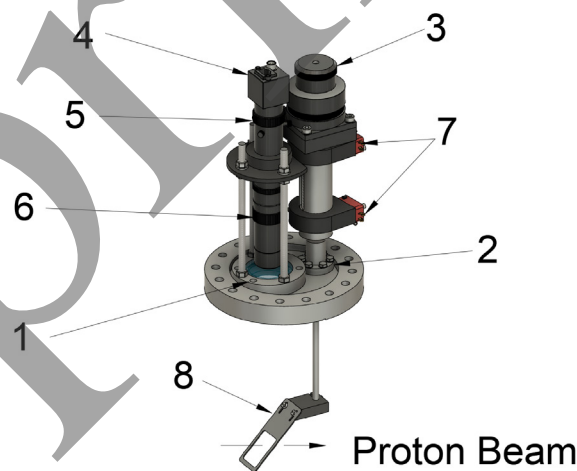


Figure 1: The optical BPM. On the CF100 is mounted the CF35 glass window (1) and the CF16 feedthrough (2) for the manipulator (3). The lens (4) of the camera (5) is shielded against stray light (6). Limit switches (7) control the position of the holder with the scintillating material (8).

CAMERA AND READOUT

The monochrome camera Blackfly S, model BFS-PGE-13Y3M-C (Edmund Optics [8]) was chosen because of a good price/performance ratio. The quantum efficiency of the CMOS sensor is above 50% in the region from 475 nm to 650 nm, providing excellent sensitivity over a broad range of wavelength. The CMOS sensor has 1.3 Megapixels (1280 x 1024) with a pixel size of about 20 μm . The resolution of the on-chip ADC is 10bit. The maximum read-out rate is 85 images per second, well suitable for live observation of the beam spot when tuning the beam. The VZM™ 100i Zoom Imaging Lens [9] was chosen, because it has a field of 26 x 26 mm, a focus distance of 175 mm with a large working tolerance of ± 3 mm.

[†]denker@helmholtz-berlin.de

The readout of the camera is done with a slightly modified LabVIEW code used also for the 2D camera. The program changes the grey scale image of the camera to false colours, provides line scans in x- and y-axis, estimates the full width half maximum (FWHM) of the beam spot, and displays its off-set of the central axis.

SCINTILLATORS

The following materials have been investigated as potential candidates for the BPMs:

- Perlux, a commercial x-ray converter foil ($\text{Gd}_2\text{O}_2\text{S:Tb}$) (PERLUX).
- Aluminium oxide AF 995 R (Desmarquest).
- P-47 Scintillator powder (SPI supplies): Yttrium-Orthosilicate Y_2SiO_5 doped with Ce^{+3} [10].
- TEM Screen Recoating Phosphor Powder (SPI supplies): 99% ZnS with Cu and Al [11].

Scintillator Preparation

The x-ray converter foil from the company PERLUX consists of a support material, covered with a reflective layer, the scintillation material and a final coating for protection of the scintillator. This makes the foil overall quite thick (2 mm). The desired size was cut out and mounted to the holder frame. The 1 mm thick AF 995 R was laser cut and mounted.

For the P-47 and the TEM powder a Kapton adhesive foil was glued to the holder frame. Kapton foil has been used for decades at the accelerator as beam exit window to separate the vacuum of the beam line from ambient air. Up to now, no beam damage to the foil has been observed. A small powder volume of 32.7 mm^3 covered the area within the holder frame abundantly. The holder is first moved manually, then mounted on a glass plate and vibrated for one minute in an ultrasonic bath (Transsonic 460, Elma) to distribute the powder evenly over the area. A 3D printed stamp with the same shape as the inner part of the holder is pressed with 6 N on the scintillator on the Kapton foil. Finally, the holder is again placed in the ultrasonic bath, this time with the powder side looking down to remove superfluous, non-sticking scintillator material. The thickness of the scintillator foils is then 0.07 mm.

Vacuum tests were performed for the Perlux foil and the powder-based scintillators. With the Perlux foil in the test chamber a vacuum of $1.5 \cdot 10^{-7} \text{ mbar}$ could be reached after 24 hours. However, there is some concern about degassing of the various layers when hit by the proton beam in vacuum. For the powder-based foils, the vacuum after 24 hours was $1.2 \cdot 10^{-7} \text{ mbar}$.

Photoluminescence Measurements

Using the LabRAM HRvolution Spectrometer (Horiba) photoluminescence measurements for the scintillators were performed. The Perlux foil shows an emittance maximum at around 530 nm. The TEM powder had one emittance maximum at 595 nm. The P47 had one maximum at 523 nm and another, about twice as high, at 797 nm. For the latter peak the quantum efficiency of the camera is about 30%. All other peaks are at wavelengths where the

quantum efficiency of the camera is more than 50%. The AF 995 R had a maximum at 690 nm, yielding a quantum efficiency of 45%, which was considered sufficient.

TESTS WITH BEAM IN AIR

Before mounting the BPMs in the beamline, they were tested at the experimental station in air. This allowed a rapid change of the scintillators without the need of breaking vacuum.

Focused Beam

Table 1 gives the FWHM observed with the four different scintillator materials for identical beam tuning. The beam was tuned to a 2.1 mm round spot with intensities below 0.5 nA observed by the 2D camera. As expected, the FWHM of the luminescence spots is larger for the two thick scintillators, the AF 995 R and the Perlux foil, as their thicker luminescence layer is now irradiated under 45° with respect to the beam. Both showed a high light intensity when exposed to the beam. The AF 995 R exhibited an afterglow, which made beam tuning difficult: Steering the beam in one axis looked first like defocusing the beam, only after some seconds it was clear that the beam really was only moved in one axis. Hence, the AF 995 R was excluded as material for the BPM. Surprisingly the afterglow could even be observed 40 minutes after the beam has been switched off. For the two powder-based scintillators, the change in observed beam size is negligible. The P47 scintillators required about a factor of 2 longer exposure times as the Perlux foil and their images varied strongly from sample to sample. The TEM powder provided 80% of the light intensity of the Perlux foil and the variation between different samples was negligible.

In the new beamline there may be up to 15 m between the BPM for visualisation of the beam and the Faraday Cup for measuring its intensity. To investigate the effect of the scintillators on the beam, the 2D camera was mounted 40 cm behind the foils. The increase in beam diameter was converted to scattering angle. Again, as expected, the increase is larger for the thicker scintillators and small for the powder-based ones.

Table 1: Observed FWHM and Scattering Angle

Scintillator	FWHM [mm]	Scattering Angle [mrad]
AF 995 R	2.95	9.93 ± 0.09
Perlux	2.33	9.05 ± 0.09
TEM powder	2.19	1.75 ± 0.08
P47	2.09	1.50 ± 0.08

Broad Beam

In a second step, the beam was broadened to a homogeneous beam profile using the same scattering foil 8 m upstream of the beamline which is employed for tumour therapy. A $10 \times 10 \text{ mm}$ square aperture was used to define the beam size. Figure 2 shows the results of the two powder-based scintillators in comparison to the Perlux foil. The

best homogeneity is provided by the Perlux foil while the P47 exhibited hot spots and cold areas. For this reason, the P47 was excluded as material. The image of the TEM powder still shows some hot spots, but they are small compared to the beam size and can therefore be eliminated by averaging.

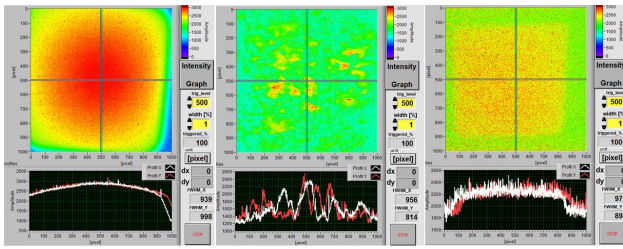


Figure 2: Screenshots of three scintillators in a broad beam. Perlux foil (left), P47 (middle) and TEM powder (right).

TEST WITH BEAM IN VACUUM

Both the BPM with the Perlux foil as well as with the TEM powder were installed in the high energy beamline of the cyclotron. However, due to time constraints, it was impossible to change the BPMs while keeping the accelerator settings. The Perlux foil could be used up to beam intensities of up to 5 nA, but its main purpose was for comparison. Figure 3 shows the first beam profile since installation of the cyclotron of a 68 MeV proton beam in the high-energy beamline. The picture was taken after the first 90° magnet and shows a broad beam in x and a narrow beam in y as expected from beamline calculations and measurements with heavy ions. Usually, for the 68 MeV protons a DC beam is injected into the cyclotron which makes it impossible to tune the beam for single turn extraction. The optical BPM now visualizes the multi-turn extraction. By changing of trim coil settings and main field, it is now possible to optimize the beam.

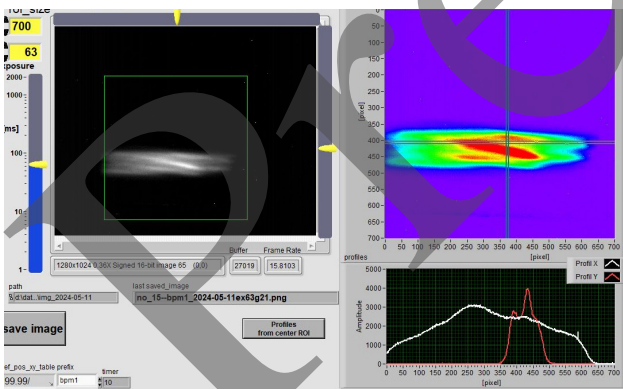


Figure 3: Screenshot and first visualisation of a 68 MeV proton beam after the first 90° magnet on the high-energy side of the cyclotron. Scintillator material: Perlux.

INSTALLATION IN NEW BEAMLINE

After the successful tests in vacuum, four more optical BPMs were produced and installed in the new beamline. Radiation safety measurements are required to obtain the operation licence for beamline extension. This beamtime was used also to commission the beamline [12] and to observe the beam spot at various positions in the beamline

(Fig. 4). For aligning the beam in the new beamline, beam intensities below 1 nA were used. This low intensity is achieved by inserting a pepper pot upstream of the cyclotron, thus maintaining the full beam emittance.

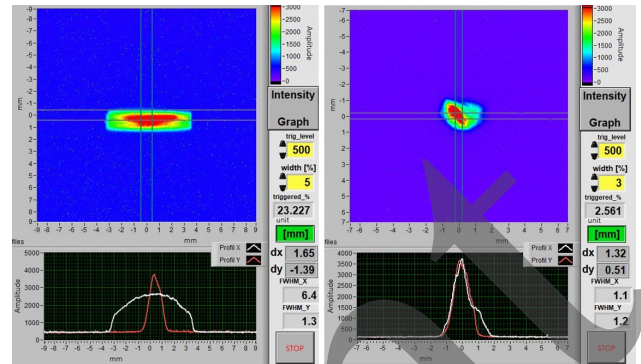


Figure 4: Screenshots of a 68 MeV proton beam on the new BPMs in the high-energy beamline of the cyclotron. Scintillator material: TEM powder. Left: in the transport section of the beamline. Right: in front of the target station.

The observation on the new BPMs matched well the predictions from the beamline calculations. In the section between the first and the second dipole leading to a target station, the beam is wider in x due to the energy dispersion of the beam. This is compensated by the second dipole so that in front of the target station a round beam spot is achieved.

CONCLUSION

Four different scintillator materials have been investigated for the use as optical BPMs. Albeit the AF 995 R and the Perlux foil provided intense images at low beam intensities, their impact on beam size excluded them for this purpose. The P47 showed large inhomogeneities in the broad beam, making it unsuitable at the end. The TEM powder provided reasonable intensity and small impact on the beam and was therefore chosen as material for the BPMs. A patent has been filed for the production method.

First tests of the optical BPMs in the beamline have been successfully performed. Overall, five of the new optical BPMs have been produced and installed at the focal points of the new beamline. Without them, the commissioning of the new beamline for the MINIBEE project [5,6] would be impossible. Up to now, no degradation on the optical BPMs have been observed.

REFERENCES

- [1] K.H. Maier, "Status of the VICKSI Project", in *Proc. CYCLOTRONS'75*, Zürich, Switzerland, Aug. 1975, pp. 68-75.
<https://proceedings.jacow.org/c75/papers/a-08.pdf>
- [2] R. Michaelsen and E. Seidel, "Modification of the VICKSI beam profile monitor system for application at low beam intensities", *Nucl. Instrum. Methods Phys. Res. A*, vol. 268, pp. 503-505, 1988.
[doi:/10.1016/0168-9002\(88\)90567-0](https://doi.org/10.1016/0168-9002(88)90567-0)

- [3] A. Denker *et al.*, “Status of the HZB Cyclotron”, in *Proc. CYCLOTRONS'22*, Beijing, China, Oct. 2022, pp. 159-162, 2022. doi:10.18429/JACoW-CYCLOTRONS2022-WEA004
- [4] A. Denker *et al.*, “Visualization of beam position and beam shape”, *Nucl. Instrum. Methods Phys. Res. B*, vol. 533, pp. 165405, 2024. doi:10.1016/j.nimb.2024.165405
- [5] A. Rousseti *et al.*, “Preclinical proton minibeam radiotherapy facility for small animal irradiation”, in *Proc. IPAC'23*, Venice, Italy, May 2023, pp. 4522-4524. doi:10.18429/JACoW-IPAC2023-THPL043
- [6] A. Rousseti *et al.*, “Current status of MINIBEE: minibeam beamline for preclinical experiments on spatial fractionation in the FLASH regime”, in *Proc. IPAC'24*, Nashville, USA, May 2024, pp. 3663-3666. doi:10.18429/JACoW-IPAC2024-THPR62
- [7] Allectra GmbH, <https://www.allectra.com/products/612-cld50-sm-c16/>
- [8] Edmundoptics, <https://www.edmundoptics.de/p/bfs-pge-13y3m-c-poe-gige-blackflyr-s-monochrome-camera/40197/>
- [9] Edmundoptics, <https://www.edmundoptics.com/p/vzmtrade-100i-zoom-imaging-lens/16469/>
- [10] SPI supplies, <https://www.2spi.com/item/04165-ab/>
- [11] SPI supplies, <https://www.2spi.com/item/04129-ab/>
- [12] J. Bundesmann *et al.*, “Commissioning of a new Beamline for Medical Research and Radiation Hardness Testing”, presented at the 17th International Particle Accelerator Conf. (IPAC'26), Deauville, France, May 2026 paper TUP8007, this conference.

Preprint